Published in final edited form as:
Biomacromolecules. 2014 March 10; 15(3): 908–914. doi:10.1021/bm4017594.

Hydrophobic drug-triggered self-assembly of nanoparticles from silk-elastin-like protein polymers for drug delivery

Xiao-Xia Xia[a,†], **Ming Wang**[b,†], **Yinan Lin**[b], **Qiaobing Xu**[b], and **David L. Kaplan**[b,*]

[a]State Key Laboratory of Microbial Metabolism, School of Life Sciences and Biotechnology, Shanghai Jiao Tong University, 800 Dong-Chuan Road, Shanghai, 200240, China

[b]Department of Biomedical Engineering, Tufts University, 4 Colby Street, Medford, Massachusetts 02155, United States

Abstract

Silk-elastin-like protein polymers (SELPs) combine the mechanical and biological properties of silk and elastin. These properties have led to the development of various SELP-based materials for drug delivery. However, SELPs have rarely been developed into nanoparticles, partially due to the complicated fabrication procedures, nor assessed for potential as an anticancer drug delivery system. We have recently constructed a series of SELPs (SE8Y, S2E8Y and S4E8Y) with various ratios of silk to elastin blocks and described their capacity to form micellar-like nanoparticles upon thermal triggering. In this study, we demonstrate that doxorubicin, a hydrophobic antitumor drug, can efficiently trigger the self-assembly of SE8Y (SELPs with silk to elastin ratio of 1:8) into uniform micellar-like nanoparticles. The drug can be loaded in the SE8Y nanoparticles with an efficiency around 6.5% (65 ng doxorubicin/μg SE8Y), S2E8Y with 6% and S4E8Y with 4%, respectively. *In vitro* studies with HeLa cell lines demonstrate that the protein polymers are not cytotoxic (IC_{50}>200μg/ml), while the doxorubicin-loaded SE8Y nanoparticles showed a 1.8-fold higher cytotoxicity than the free drug. Confocal laser scanning microscopy (CLSM) and flow cytometry indicate significant uptake of the SE8Y nanoparticles by the cells, and suggest internalization of the nanoparticles through endocytosis. This study provides an all-aqueous, facile method to prepare nanoscale, drug-loaded SELPs packages, with potential for tumor cell treatments.

Keywords

silk-elastin-like protein polymers; self-assembly; doxorubicin; nanoparticles; drug delivery

1. Introduction

During the past three decades, sophisticated drug delivery systems have been developed in order to improve therapeutic outcomes. These systems reduced toxic side effects and decreased the number of time required for drug administration, while improving cellular

*Corresponding author: David L. Kaplan, Ph.D; Tufts University, Department of Biomedical Engineering, 4 Colby Street, Medford, Massachusetts, 02155, USA. Phone: +1-617-627-3251; Fax: +1-617-627-3231; david.kaplan@tufts.edu.
†These authors contributed equally to this work.

uptake and bioavailability.[1, 2] Nanoparticulate carriers in particular have been extensively investigated as a platform for controlled drug delivery.[3, 4] In general, the material employed as a carrier should offer control of structure, morphology and function, while also exhibiting good mechanical stability.[5] Therefore, biodegradable and non-cytotoxic polymers are preferred, such as many synthetic (aliphatic polyesters, poly-glycolic acid (PGA), polylactic acid (PLA) and genetically engineered (poly-peptides and proteins) polymers, which have been employed for encapsulation, and the incorporation or binding of active compounds.[6, 7]

Although synthetic polymers offer the potential of controlling the release of the encapsulated therapeutic agent over time, they typically demand organic solvents or relatively harsh formulation conditions during processing, resulting in negative impacts on biocompatibility due to residual toxic solvents or the generation of acidic degradation products.[8] In recent years, genetically engineered protein polymers consisting of repeating amino acid sequence motifs from natural structural proteins or of *de novo* design, have been developed and evaluated as matrices for controlled drug delivery. In comparison with chemically synthesized polymers, genetic engineering of recombinant proteins has enabled the design of protein biomaterials with uniform composition, precise molecular weight and correlation of structure-function relationships for use in drug delivery.[9, 10] The repeating blocks of amino acids, responsible for distinct mechanical, chemical, and biological properties of many natural proteins, like collagen, silk, and elastin have been widely used as design motifs. For example, various elastin-like peptides have been constructed as block co-polymers to form spherical micellar nanoparticles upon coacervation for drug delivery, [11–13] and lysine-modified chimeric spider silk proteins have been designed to generate nanoparticles for gene delivery.[14] In addition, by combining polypeptide sequences derived from silk and elastin, a series of silk-elastin-like protein polymers (SELPs) displaying unique mechanical properties have been produced. Notably, the silk-like domains of these protein polymers are able to crystallize into β-sheets *via* inter/intramolecular hydrogen bonding as physical crosslinks (hard blocks). In turn, the elastin-like blocks can decrease the overall crystallinity of the polymer and thus enhance the solubility of SELPs (soft blocks). Compared with elastin-based materials, the silk blocks in SELPs enable robust materials formation without the need to introduce crosslinking agents. Through tuning the ratio of silk and elastin blocks, material strength, stimuli-sensitivity, biodegradation, and drug and gene release profiles of SELPs can be precisely controlled. [15–18] In summary, SELPs form materials with unique mechanical properties, avoid a need for chemical crosslinking, can be processed in aqueous conditions, and have been evaluated as controlled drug release devices for a variety of biomedical applications.

Despite significant advances made with SELPs for drug/gene delivery, they have primarily been used for direct injection into tumors, which limits the broader application of these polymers.[16] Developing SELPs into nanoparticles that can systemically administer drugs to target sites would be advantageous. Recently, Anumolu *et al*. generated highly uniform SELPs nanoparticles using an electrospray droplet evaporation technique and showed these nanoparticles encapsulated model therapeutic agents. However, the applied preparation technique is relatively sophisticated with limits to scalability.[19, 20] We have earlier reported the design of three recombinant silk elastin-like protein polymers (SE8Y, S2E8Y, S4E8Y)

with silk (GAGAGS) to elastin block (GXGVP) ratios at 1:8, 1:4, and 1:2, respectively. These polymers spontaneously formed, or by thermal triggering, self-assemble into micellar-like nanoparticles either reversibly or irreversibly.[21]

The aim of the present study was to investigate the applicability of genetically engineered SELP (SE8Y, S2E8Y, S4E8Y) nanoparticles as drug carriers. First, the hydrophobic molecule 1-anilinonaphthalene-8-sulfonic acid (1,8-ANS) was studied to determine the critical micelle concentration (CMC) and loading capacities of these protein polymers. Next, doxorubicin was loaded into the SELPs nanoparticles to characterize size and properties. Further, the cytotoxicity and cellular uptake of doxorubicin-encapsulated SELP nanoparticles against Hela cells was investigated.

2. Materials and Methods

2.1 Materials

All chemical reagents were purchased from Fisher Scientific, Inc. (Pittsburgh, PA) or Sigma-Aldrich (St. Louis, MO). Dulbecco's phosphate-buffered saline (PBS), 3-(4,5-dimethylthiazol-2-yl)-2,5-diphenyltetrazolium bromide (MTT), Dulbecco's Modified Eagles's Medium (DMEM) and Fetal bovine serum (FBS) were purchased from Invitrogen (Carlsbad, CA). Doxorubicin hydrochloride was obtained from LC laboratories (Woburn, MA). To convert the drug into the hydrophobic form, doxorubicin hydrochloride was neutralized by phosphate buffer solution (0.1 M, pH 8.5) followed by centrifugation. The solid pellet was washed with water and lyophilized for drug loading experiment. Nickel-chelated sepharose resin was purchased from Qiagen (Valencia, CA). Methods used for the synthesis of silk-elastin-like protein polymers (SE8Y, S2E8Y and S4E8Y) with silk to elastin ratios at 1:8, 1:4, and 1:2, and molecular weights of 55.7 kDa, 53.0 kDa and 47.8 kDa, respectively, have been described previously.[21] The amino acid sequences of SE8Y is $[(GAGAGS)(GVGVP)_4(GYGVP)(GVGVP)_3]_{14}$, S2E8Y is $[(GAGAGS)_2(GVGVP)_4(GYGVP)(GVGVP)_3]_{12}$ and S4E8Y is $[(GAGAGS)_4(GVGVP)_4(GYGVP)(GVGVP)_3]_9$. The purified proteins were dialyzed against deionized water for 5 days using Slide-A-Lyzer Dialysis cassettes (MWCO 3.5 kDa, Thermo Scientific) and then concentrated using Amicon® Ultra-15 centrifugal filter units with Ultracel-30 membranes (Millipore, Billerica, MA). Protein concentrations were measured using a Pierce BCA Protein Assay kit (Product # 23225; Thermo Scientific, Rockford, IL) and the purity of the proteins was monitored via sodium dodecyl sulfate polyacrylamide gel electrophoresis (SDS-PAGE).

2.2 Fluorescence spectroscopy of protein polymers mixed with 1,8-ANS and critical micelle concentration (CMC) measurement

Fluorescence measurements were performed using a Hitachi F-4500 fluorescence spectrophotometer equipped with a water-circulator cooled cell jacket. The 1,8-ANS was used as a hydrophobic fluorescent probe. Stock solutions of SELPs (10mg/ml) and 1,8-ANS (8mM) prepared with PBS were mixed together at various concentrations for the SELPs and 80 μM for 1,8-ANS. The mixture of SELPs and fluorescent probe was incubated at 25°C for

10 min and emission spectra were measured three times at an excitation wavelength of 370 nm.

From the 1,8-ANS excitation spectra, the fluorescence intensity was plotted against the logarithm of the protein concentrations. The CMC was determined based on the crossover point at low concentration on this plot.[22]

2.3 Preparation of drug loading micellar-like nanoparticles

One mg doxorubicin was dissolved in 1 ml silk-elastin-like protein polymer solution (1 mg/ml) and incubated at room temperature (25°C) for 8h under dynamic conditions (20rpm). The drug-containing solution was then centrifuged at 6000×*g* for 10 min to remove undissolved drug. The supernatant was positioned into a Slide-A-Lyzer Dialysis Cassette (MWCO 3.5 kDa, Thermo Scientific) and then subjected to dialysis against 1 L of distill water for 24 h to remove unloaded drugs. The water was refreshed every 4 h. The loading amount of doxorubicin was measured by UV absorbance at 480nm, using a standard calibration curve experimentally obtained. The drug loading efficiency (DLE) was defined as follow: DLE= (mass of drug loaded in micelles/mass of drug-loaded micelles)×100%.

2.4 Characterization of drug-loaded SELPs nanoparticles

Dynamic Light Scattering (DLS) was carried out on a DynaPro Titan instrument (Wyatt Technology, Santa Barbara, CA) equipped with a temperature controller. Drug loading protein solutions (0.2 mg/ml) were filtered through a 0.45 μm filter prior to DLS measurements that were carried out at a fixed scattering angle of 90° at 25 and 37°C, respectively. The samples were stabilized at the desired temperature for 10 minutes prior to measurement. To obtain the hydrodynamic radii, the intensity autocorrelation functions were analyzed using the Dynamics software (Wyatt Technology, Santa Barbara, CA).

The phase transition was characterized by monitoring the absorbance of drug loading solutions (1 mg/ml) at 300 nm as a function of temperature on an Aviv 14DS UV-Vis spectrophotometer equipped with a Peltier temperature controller (Aviv Biomedical, Lakewood, NJ). Absorbance readings were taken after equilibrating a solution at the desired temperature for 30 s.

Cryogenic scanning electron microscope (cryo-SEM) was used to confirm the structure of the drug-loaded protein nanoparticles. A drop (10 uL) of sample suspension was placed inside a custom-made copper holder and plunge-frozen in slushy nitrogen. After freezing, the sample was transferred under liquid nitrogen in a Leica EM VCT100 cryo transfer system (Leica Microsystems Inc., Buffalo Grove, IL) to a pre-cooled Baltec MED020 high vacuum freeze-fracture coating system (Baltec, Baltzers, Liechtenstein, Germany) at −140°C. The sample was then fractured and partially freeze-dried at −110°C for 2 min, followed by coating with a thin layer (10 nm thick) of Pt/Pd prior to imaging in a pre-cooled (−120°C) cryo-SEM (Zeiss NVision 40, Carl Zeiss SMT Inc., Peabody, MA, USA). These experiments were performed at the Center for Nanoscale Systems (CNS), a member of the National Nanotechnology Infrastructure Network (NNIN). CNS is part of the Faculty of Arts and Sciences at Harvard University.

2.5 Cytotoxicity assay

HeLa cells were purchased from ATCC (Manassas, VA) and maintained in high glucose DMEM supplemented with 10% FBS and 1% penicillin/streptomycin at 37°C in the presence of 5% CO_2. Cells were seeded in 96-well plate at a density of 10, 000 cells per well 24 h before the delivery experiments. At the day of delivery, varying doxorubicin encapsulated SELPs nanoparticles and free doxorubincin were added to cells directly. The cell viability was measured by MTT assay following a further 48 h of incubation. At the end of incubation, the cell culture medium was aspirated, and the cells were washed with PBS one time followed by incubation with 125 μL MTT solution (0.5 mg/mL in DMEM) for 4h at 37°C. The resulting formazan dyes were dissolved in 125 μL DMSO, and the absorbance of solutions was monitored at 595 nm on a SpectraMax M2 multi-mode microplate reader (Molecular Devices, Inc., Sunnyvale, CA).

2.6 Cellular uptake of doxorubicin encapsulated SELPs nanoparticles

For the confocal laser scanning microscopy (CLSM) observations, HeLa cells were seeded in culture slides (BD Falcon) at a density of 50,000 cells per vessel and incubated for 24 h. The cells were washed with PBS and incubated with doxorubicin encapsulated SE8Y (5 μM) or free doxorubicin (5 μM) in 0.5 mL DMEM medium for 40 min or 4 h. At the end of incubation, DMEM medium was aspirated, and the cells were washed with PBS two times before fixed with 3.8 % formalin solution, followed by cell nuclei staining with DAPI. The CLSM images were obtained on Axiovert 200 M inverted microscopes (Zeiss). For the FACS analysis of nanoparticle uptake, HeLa cells (10,000 cells per well) were seeded in 12-well plate a day before experiment and then incubated with doxorubicin encapsulated silk-elastin nanoparticles SE8Y for 4h (5 μM) at 4°C and 37°C, respectively. At the end of incubation, cells were harvested, washed with PBS, and resuspended in PBS for FACS analysis on FACScalibur (BD Sciences).

3. Results and Discussion

3.1 Loading of hydrophobic fluorescent molecules

In our previous study we constructed a series of silk elastin-like protein polymers (SELPs) with different ratios of silk (GAGAGS) to elastin (GXGVP) blocks and found these protein polymers could spontaneously form micellar-like nanoparticles.[21] The assembly capability of SELPs depended on the silk to elastin ratio. In the current study using these proteins, we assessed the capacity of the nanoparticles to uptake hydrophobic molecules to investigate whether they could be used as a drug delivery system. The three recombinant SELPs (SE8Y, S2E8Y, S4E8Y) with silk to elastin block ratios at 1:8, 1:4, and 1:2, were expressed and purified and the purity of the proteins was verified by SDS-PAGE (Fig. 1). Next, a hydrophobic fluorescent molecule, 1,8-ANS was introduced into the three protein solutions, respectively. Notably, 1,8-ANS fluoresces in a hydrophobic environment and has often been used to investigate the capacity of amphiphilic block copolymers to encapsulate hydrophobic drugs.[12, 22] The fluorescent spectra of 1,8-ANS with 0.5 mg/ml SE8Y, S2E8Y and S4E8Y protein solutions at 25°C is shown in Figure 1. The wavelengths of the emission peaks for SE8Y and S2E8Y were 475±3nm, and for S4E8Y was 509±3nm. The blue shift of the emission peak indicated the microscopic environments around 1,8-ANS were more

hydrophobic.[23] The fluorescence intensity of SE8Y at 475±3nm was around 2-fold higher than that of S2E8Y and 8-fold higher than S4E8Y, which indicated that the loading capacity of the hydrophobic molecule of SE8Y was significantly higher than that of S2E8Y and S4E8Y. This result may be related to the physical properties of the original proteins. Before adding 1,8-ANS, S4E8Y already formed a number of micellar-like nanoparticles with a dense cross-linked silk core, [21] which might hinder the diffusion of the 1,8-ANS into the particles. In contrast, SE8Y solution was dominated by the free chains of the protein. The addition of 1,8-ANS might trigger the formation of micellar-like nanoparticles due to the change of hydrophobicity, leading to higher amounts of 1,8-ANS encapsulated into the particles. To verify this, the fluorescence spectra of urea (denaturant) added to SE8Y/ANS was also examined. As expected, the assembled structures were disrupted by urea as the fluorescence intensity dramatically decreased. To exclude the possibility of fluorescence of SELPs themselves, the protein solution of SE8Y was also included as a control (Fig. 1).

Furthermore, the fluorescence intensity increased with the concentration of the protein polymers, which is consistent with the notion that an increased number of micellar-like nanoparticles in the solution leads to a larger reservoir for the hydrophobic fluorophore. From the plot of fluorescence intensity versus protein polymer concentration, an abrupt increase of fluorescence value at 475nm can be detected upon increasing protein polymer concentrations, indicating the formation of micelles and the transfer of 1,8-ANS into the micellar-like nanoparticles (Fig. 2a–c). As illustrated in Fig. 2d, the critical micelle concentration (CMC) for the SE8Y and S2E8Y was 0.125 mg/ml (2.24 μM) and 0.25 mg/ml (4.72 μM), respectively (Fig. 2d), which is in agreement with the formation of stable micellar structures.[23] S4E8Y did not show an abrupt increase of fluorescence upon increasing protein concentrations, indicating few particles formed. In summary, SE8Y showed the highest loading capacity for 1,8-ANS and the lowest CMC value.

3.2 Preparation of drug loading protein nanoparticles

Next, we examined the ability of these SELPs to serve as a potential drug delivery system. Hydrophobic drug doxorubicin was added to SELPs solution followed by micellization at 25°C. The drug loading efficiency value of SE8Y was 6.5 %, whereas S2E8Y was 6% and S4E8Y was 4%. Notably, the difference in encapsulation efficiency of doxorubicin between SE8Y and S4E8Y was less than 2 fold, whereas the difference in the encapsulation of 1,8-ANS was reaching 8 fold. This could be explained by their different encapsulation mechanism and measurement method. The average hydrodynamic radii (Rh) of Dox-loaded nanoparticles were 50±10 nm (SE8Y), 72±11 nm (S2E8Y) and142±10 nm (S4E8Y), respectively (Fig. 3a). Before adding Dox, the average Rh of SE8Y was only 5.2±1.8 nm, which is suggestive of free chains. This result demonstrated that Dox triggered the self-assembly of SE8Y into nanoparticles (Fig. 3b), the same as 1,8-ANS. Most importantly, these triggers might be expanded to other hydrophobic molecules. The average Rh of S2E8Y and S4E8Y were 29±9.8 nm and 89±7.3 nm, respectively, which was much smaller than that of Dox-loaded nanoparticles. This might be due to the hydrophobic association of small particles into larger ones. Notably, when we added hydrophilic doxorubicin hydrochloride into SELPs protein solutions, much less doxorubicin was encapsulated into the protein nanoparticles (DLE<0.1%), which indicated that hydrophobic interaction played

a dominant role in the encapsulation process instead of other interactions including hydrogen bonding etc.

When Dox-loaded nanoparticles of SELPs were incubated at 37°C (physical temperature), the average Rh of SE8Y particles increased to 139±1.8 nm. In contrast, the sizes of nanoparticles of S2E8Y and S4E8Y did not change significantly. This might be explained by the lower phase transition temperature (~35°C) of drug-loaded SE8Y (Fig. 3c). Notably, the phase-transition temperature (T_t) of the SELPs was significantly altered following encapsulation of doxorubicin. T_t value is typically modulated by varying the hydrophobicity of the guest residue (X) of the elastin blocks, whereby hydrophobic guest residues depress the T_t value, and hydrophilic residues elevate the T_t value.[23–25] In a similar manner, the encapsulation of hydrophobic molecules might increase the hydrophobicity of protein solutions, thus down-regulating the T_t. To directly visualize the morphology and shape diversity of the Dox-loaded SE8Y nanoparticles, we imaged the samples by cryogenic scanning electron microscope (cryo-SEM). SEM imaging confirmed the morphology of Dox-loaded nanoparticles that displayed uniform spheres ranging from 250 nm to 300 nm in average diameter, which was consistent with that determined by DLS (Fig. 3d).

The stability of drug-loaded SE8Y nanoparticles under physiological conditions was also examined. The size of drug-loaded SE8Y nanoparticles in phosphate buffer saline supplemented with 10% FBS at 37°C for 48h remained constant (Fig. 4) although the polydispersity increased a little, which allows the potential application of the SELPs for in vivo chemotherapy drug delivery.[26] The stability of these nanoparticles might be due to the physical cross-linking of silk units in SELPs, which avoids the need to introduce other cross-linking agents.

3.3 In vitro cytotoxicity

As a good drug delivery vehicle, low cytotoxicity of the vehicle itself is essential for practical applications.[27, 28] Cytotoxicity of SELPs *in vitro* was estimated against HeLa cells via MTT assay. As shown in Figure 5a, cell viability was still above 90% when the concentration of protein polymers was increased to 200 μg/ml, indicating the low cytotoxicity and high potential of SELPs as chemotherapy drug carrier. When the cells were treated by doxorubicin encapsulated SELPs nanoparticles, cell viability was significantly decreased in comparison with DMEM treated controls. The IC_{50} (the concentration required for 50% inhibition of cellular growth) values were determined as 0.95μM for free Dox, 0.55μM for doxorubicin encapsulated SE8Y (Dox-S1), 0.61μM for doxorubicin encapsulated S2E8Y (Dox-S2) and 1.35μM for doxorubicin encapsulated S4E8Y (Dox-S4), respectively (Fig. 5b & c). Free doxorubicin is expected to directly diffuse through the lipid bilayers into the cell and nucleus. In contrast, our slightly lower level of toxicity for Dox-S4 relative to free doxorubicin can be explained by the additional steps required for Dox-S4 to be taken up by the cells and with a complex process for drug release into the cytosol and nucleus. Thus, it is likely that 48 h may be an insufficient period for the complete release of doxorubicin from the S4/dox inside a cell. Interestingly, Dox-S1 showed a higher cytotoxicity than free drug and the other two drug-loaded SELPs. This might be explained by the controlled release of drugs leading to a higher concentration of doxorubicin entering

nuclei. However, the detailed drug release mechanism was not clear. Notably, in our study *in-vitro* release experiment could not mimic the *in-vivo* system. We tried various PBS buffers with pH 4.0 to pH 8.0 and with or without FBS for *in vitro* release experiment, but we did not find any significant release of drugs within 4 days. Only when we added some proteases like elastase, we could see small amounts of drug release. We believe that the enzymatic degradation of SELPs might contribute to the release of doxorubicin.

3.4 Cellular uptake and intracellular trafficking of Dox-loaded SE8Y nanoparticles (S1/Dox)

Due to the higher drug loading capacity of SE8Y and the cytotoxicity of its Dox-loaded nanoparticles, the intracellular trafficking and fate of S1/Dox were monitored by confocal laser scanning microscopy. CLSM images (Fig. 6) of HeLa cells treated with S1/Dox and free Dox indicated the different uptake pathways of nanoparticles and free Dox. At 40 min of incubation, free doxorubicin accumulated in cell nuclei, which is understandable because free Dox enters cells quickly via a membrane diffusion pathway. S1/Dox treated cells, however, mostly accumulated the nanoparticles in cytoplasm which might enter cells via an endocytosis pathway. A longer incubation of S1/Dox with HeLa cells facilitated the diffusion of Dox into nuclei, which may arise from the gradual intracellular release of DOX from the S1/Dox nanoparticles. We believe that the controlled release of DOX from S1/Dox could contribute to the higher delivery efficiency of SE8Y nanoparticles.[29, 30] The internalization and endocytosis of S1/DOX nanoparticles were further confirmed and studied by a FACS quantification of nanoparticle uptake. Endocytosis is known as an energy-dependent process, decreased nanoparticle internalization is usually observed at a low temperature. As shown in Figure 7, a decreased DOX fluorescence intensity was observed for cells incubated with S1-Dox at 4°C compared to that at 37°C, suggesting the low cellular uptake of S1-Dox nanoparticles at 4°C.

4. Conclusions

Engineered silk-elastin like protein polymers, triggered by hydrophobic molecules, assembled into nanoparticles with potential for use for the delivery of hydrophobic drugs. One major advantage of the system is that the nanoparticles can be produced and loaded within an all-aqueous process under ambient conditions, which is important considering encapsulation of labile compounds and the biocompatibility of the biomaterials. In addition, genetically encoded synthesis provides a simple and accurate method to control particle diameter, degree of drug loading and incorporation of other biologically active peptides. We anticipate that this hydrophobic drug triggered SELPs nanoparticle system possesses good potential for the future direction related to cancer treatments.

Acknowledgments

This work was supported by the NIH P41 Tissue Engineering Resource Center (P41 EB002520) and the Shanghai Pujiang Program (13PJ1404800). Further support by the Program for Professor of Special Appointment (Eastern Scholar) at Shanghai Institutions of Higher Learning is appreciated. This work was performed in part at the Center for Nanoscale Systems (CNS), a member of the National Nanotechnology Infrastructure Network (NNIN). CNS is part of the Faculty of Arts and Sciences at Harvard University.

References

1. Uhrich KE, Cannizzaro SM, Langer RS, Shakesheff KM. Chem Rev. 1999; 99:3181–3198. [PubMed: 11749514]
2. Frandsen JL, Ghandehari H. Chem Soc Rev. 2012; 41:2696–2706. [PubMed: 22344293]
3. Allen TM, Cullis PR. Science. 2004; 303:1818–1822. [PubMed: 15031496]
4. Saha RN, Vasanthakumar S, Bende G, Snehalatha M. Mol Membr Biol. 2010; 27:215–231. [PubMed: 20939772]
5. Altman GH, Diaz F, Jakuba C, Calabro T, Horan RL, Chen J, Lu H, Richmond J, Kaplan DL. Biomaterials. 2003; 24:401–416. [PubMed: 12423595]
6. Langer R, Peppas NA. AIChE J. 2003; 49:2990–3006.
7. Liechty WB, Kryscio DR, Slaughter BV, Peppas NA. Annu Rev Chem Biomol Eng. 2010; 1:149–173. [PubMed: 22432577]
8. Morlock M, Koll H, Winter G, Kissel T. Europ J Pharm Biopharm. 1997; 43:29–36.
9. Maskarinec SA, Tirrell DA. Curr Opin Biotechnol. 2005; 16:422–426. [PubMed: 16006115]
10. Langer R, Tirrell DA. Nature. 2004; 428:487–492. [PubMed: 15057821]
11. Kim W, Chaikof EL. Adv Drug Deliv Rev. 2010; 62:1468–1478. [PubMed: 20441783]
12. Fujita Y, Mie M, Kobatake E. Biomaterials. 2009; 30:3450–3457. [PubMed: 19324406]
13. Chilkoti A, Dreher MR, Meyer DE. Adv Drug Deliv Rev. 2002; 54:1093–1111. [PubMed: 12384309]
14. Numata K, Hamasaki J, Subramanian B, Kaplan DL. J Control Release. 2010; 146:136–143. [PubMed: 20457191]
15. Megeed Z, Cappello J, Ghandehari H. Adv Drug Deliv Rev. 2002; 54:1075–1091. [PubMed: 12384308]
16. Gustafson JA, Ghandehari H. Adv Drug Deliv Rev. 2010; 62:1509–1523. [PubMed: 20430059]
17. Hu X, Wang X, Rnjak J, Weiss AS, Kaplan DL. Biomaterials. 2010; 31:8121–8131. [PubMed: 20674969]
18. Hu X, Lu Q, Sun L, Cebe P, Wang X, Zhang X, Kaplan DL. Biomacromolecules. 2010; 11:3178–3188. [PubMed: 20942397]
19. Anumolu R, Gustafson JA, Magda JJ, Cappello J, Ghandehari H, Pease LF. ACS Nano. 2011; 5:5374–5382. [PubMed: 21696150]
20. Jaworek A. Powder Technol. 2007; 176:18–35.
21. Xia XX, Xu Q, Hu X, Qin G, Kaplan DL. Biomacromolecules. 2011; 12:3844–3850. [PubMed: 21955178]
22. Kim W, Thévenot J, Ibarboure E, Lecommandoux S, Chaikof EL. Angew Chem Int Ed Engl. 2010; 49:4257–4260. [PubMed: 20446331]
23. Urry DW, Urry KD, Szaflarski W, Nowicki M. Adv Drug Deliv Rev. 2010; 62:1404–1455. [PubMed: 20655344]
24. Urry DW, Hugel T, Seitz M, Gaub HE, Sheiba L, Dea J, Xu J, Parker T. Philos Trans R Soc Lond B Biol Sci. 2002; 357:169–184. [PubMed: 11911774]
25. Dreher MR, Simnick AJ, Fischer K, Smith RJ, Patel A, Schmidt M, Chilkoti A. J Am Chem Soc. 2008; 130:687–694. [PubMed: 18085778]
26. McDaniel JR, Bhattacharyya J, Vargo KB, Hassouneh W, Hammer DA, Chilkoti A. Angew Chem Int Ed Engl. 2013; 52:1683–1687. [PubMed: 23280697]
27. MacKay JA, Chen M, McDaniel JR, Liu W, Simnick AJ, Chilkoti A. Nat Mater. 2009; 8:993–999. [PubMed: 19898461]
28. Seib FP, Jones GT, Rnjak-Kovacina J, Lin Y, Kaplan DL. Adv Healthc Mater. 2013; 2:1606–1611. [PubMed: 23625825]
29. Ren D, Kratz F, Wang SW. Small. 2011; 7:1051–1060. [PubMed: 21456086]
30. dos Santos T, Varela J, Lynch I, Salvati A, Dawson KA. Small. 2011; 7:3341–3349. [PubMed: 22009913]

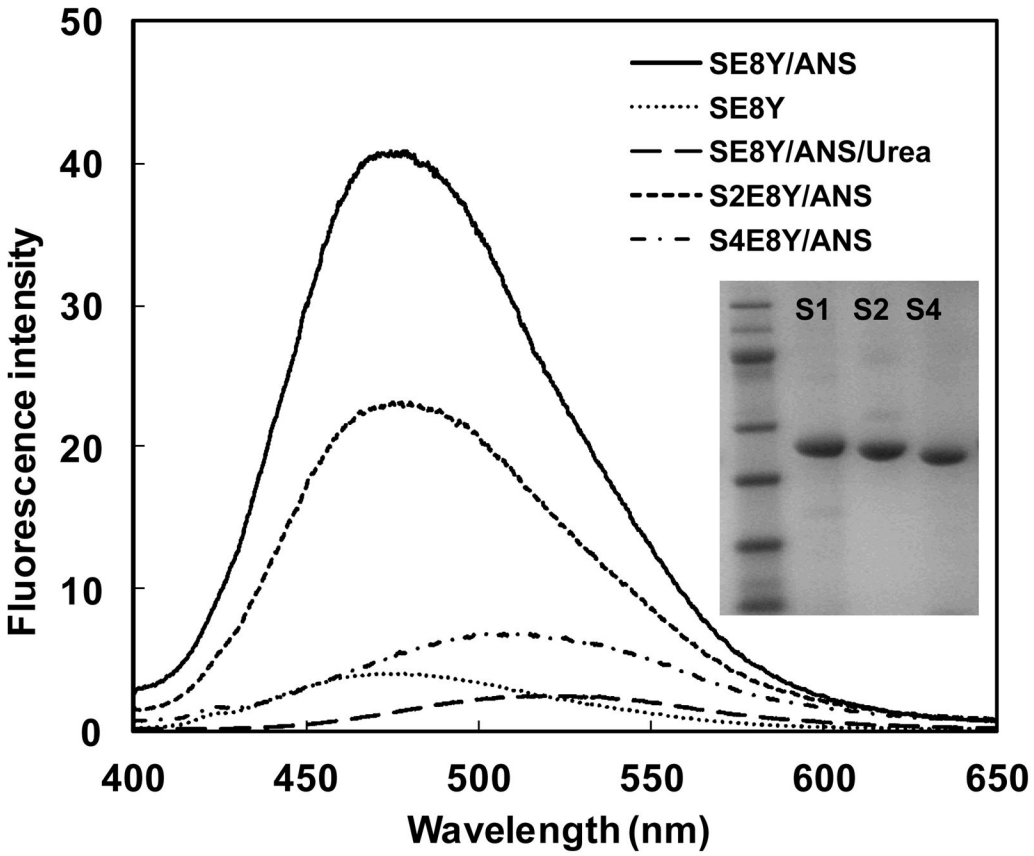

Fig. 1.

Fluorescence spectra of 1,8-ANS (80μM) with 0.5mg/ml SE8Y, S2E8Y and S4E8Y in phosphate buffer saline at 25 °C. Fluorescence spectra of SE8Y and SE8Y in 8M urea solution were included for controls. The inset shows the SDS-PAGE gel analysis of purified SE8Y, S2E8Y and S4E8Y proteins.

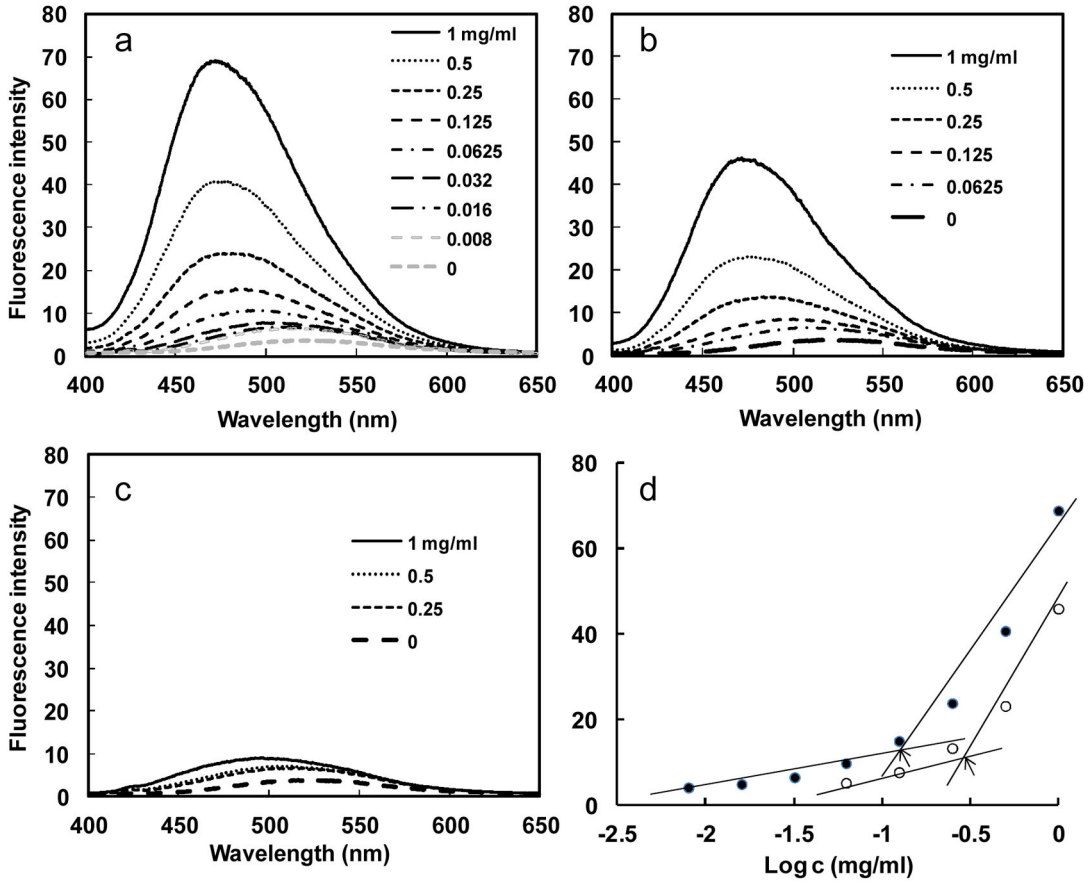

Fig. 2.

Fluorescence spectra of 1,8-ANS (80μM) with various concentration of SE8Y (a), S2E8Y (b) and S4E8Y (c) in phosphate buffer saline at 25°C. d) Fluorescence intensity of 1,8-ANS as a function of the logarithmic concentration of the SE8Y (close dot) and S2E8Y (open dot). Arrows indicate the critical micellar concentrations.

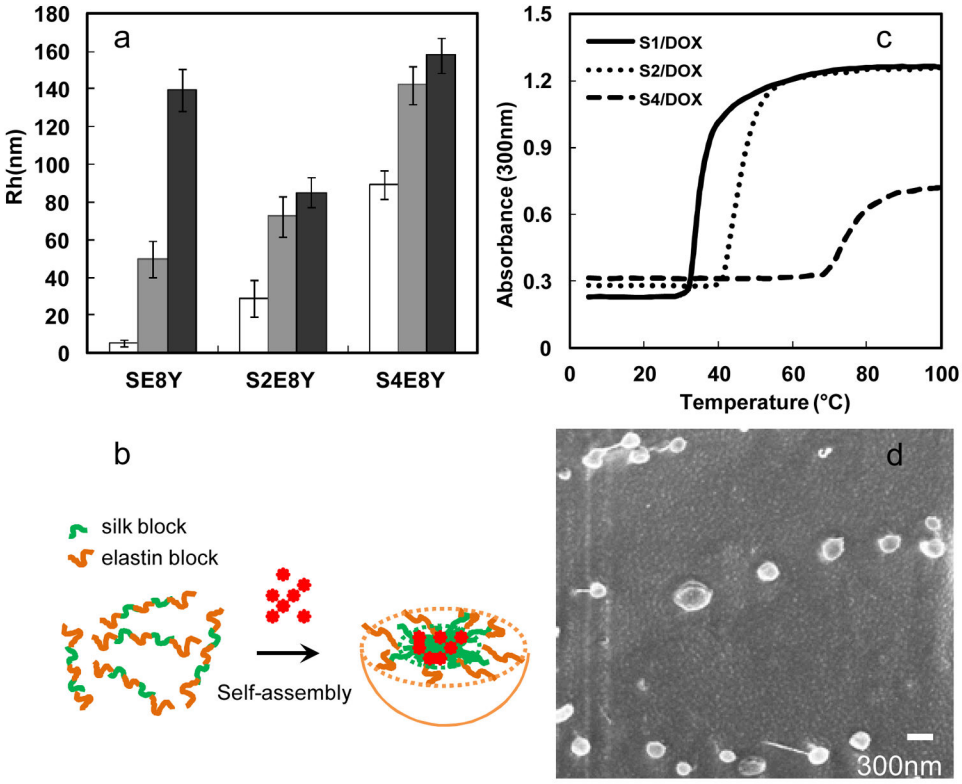

Fig. 3.

Characterization of doxorubicin-encapsulated nanoparticles. a) Sizes of SE8Y/Dox, S2E8Y/Dox and S4E8Y/Dox complexes at 25°C (gray bar) and 37°C (black bar) with respective protein solutions as controls (white bar). b) Turbidity profiles of the SE8Y/Dox (S1/Dox), S2E8Y/Dox (S2/Dox) and S4E8Y/Dox (S4/Dox) complexes at 1 mg/mL as a function of temperature. c) Doxorubicin-triggered self assembly of SE8Y into micellar-like nanoparticles. d) Representative cryogenic scanning electron microscope (cryo-SEM) of Dox-loaded SE8Y nanoparticles.

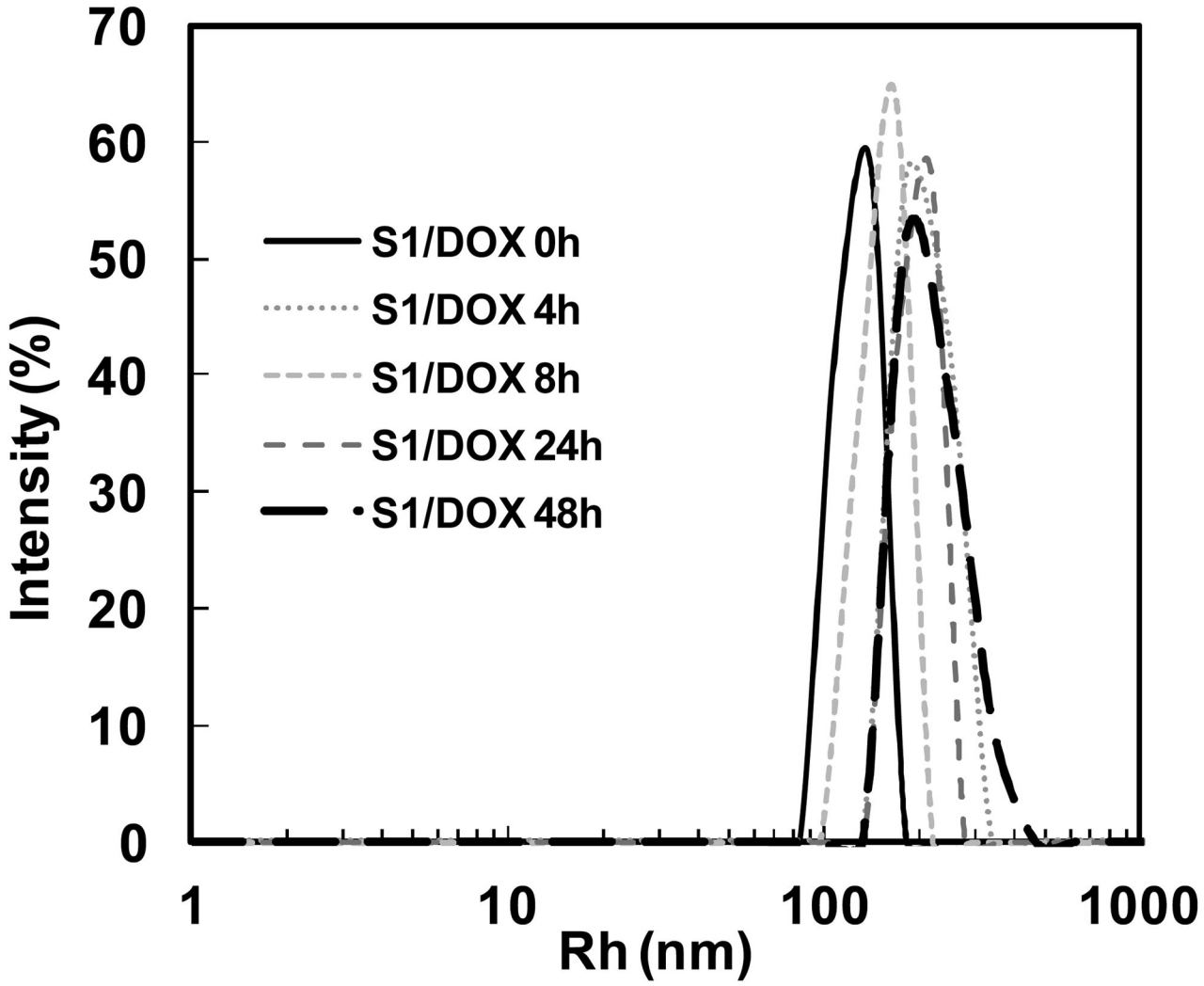

Fig. 4.

DLS size distribution profiles for doxorubicin encapsulated SE8Y (S1/Dox) nanoparticles in phosphate buffer saline with 10% FBS at 37°C over time.

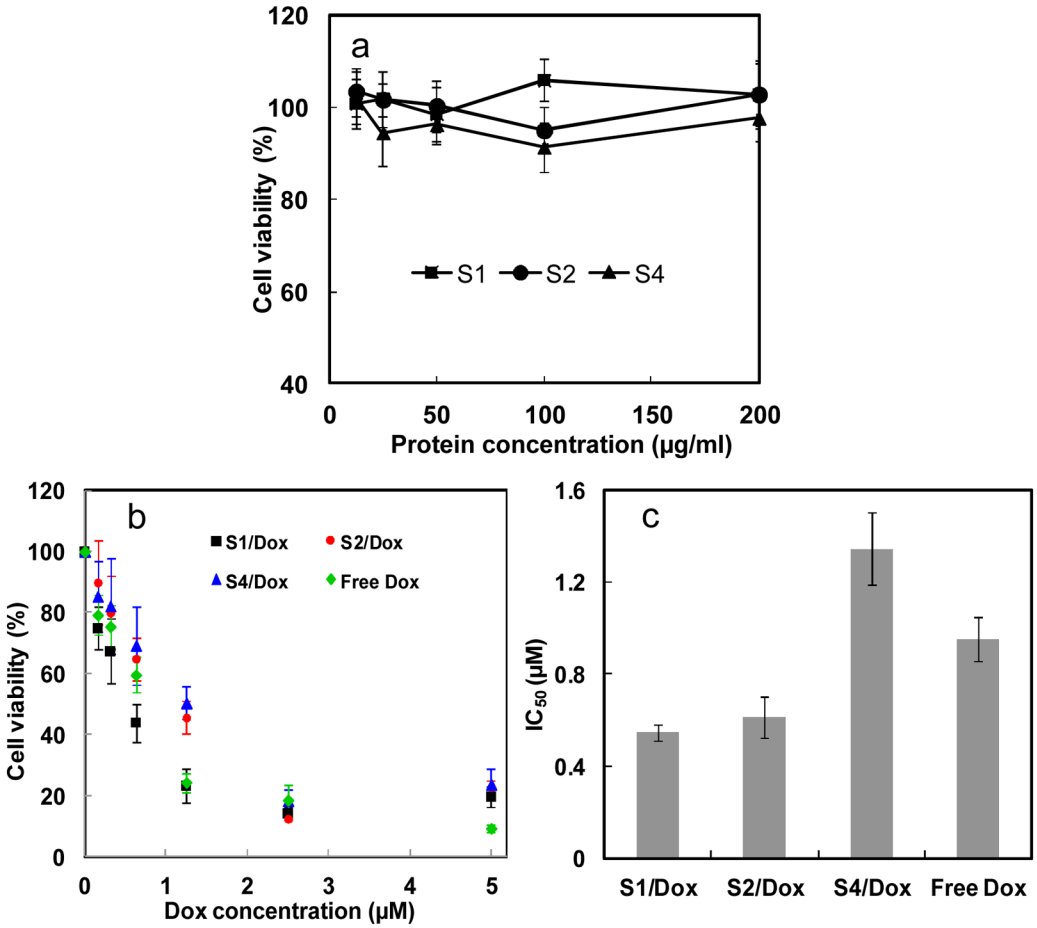

Fig. 5.

a) Cytotoxicity of the SE8Y (S1), S2E8Y (S2) and S4E8Y (S4) protein polymers against Hela cells. b) *In vitro* cytotoxicity of SE8Y/Dox (S1/Dox), S2E8Y/Dox (S2/Dox), S4E8Y/Dox (S4/Dox) complexes and free doxorubicin against HeLa cells. c) IC_{50} values of S1/Dox, S2/Dox, S4/Dox complexes and free doxorubicin against HeLa cells.

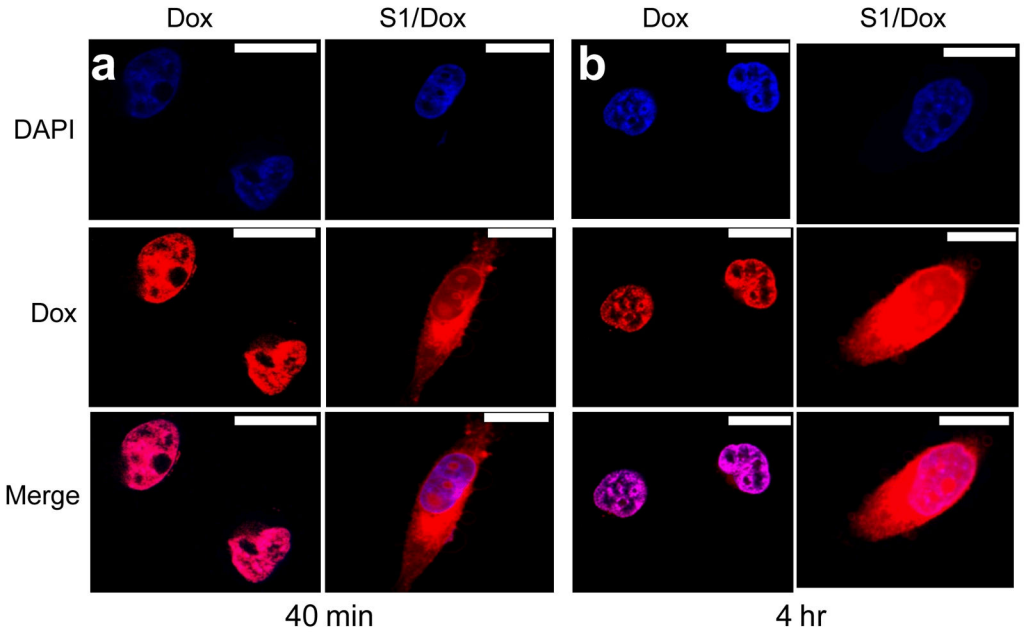

Fig. 6.

Delivery of doxorubicin into HeLa cells via SE8Y nanoparticles with different times: a) 40 min and b) 4h by CLSM. Nucleus was stained with DAPI (blue signal). The scale bar is 10 μm.

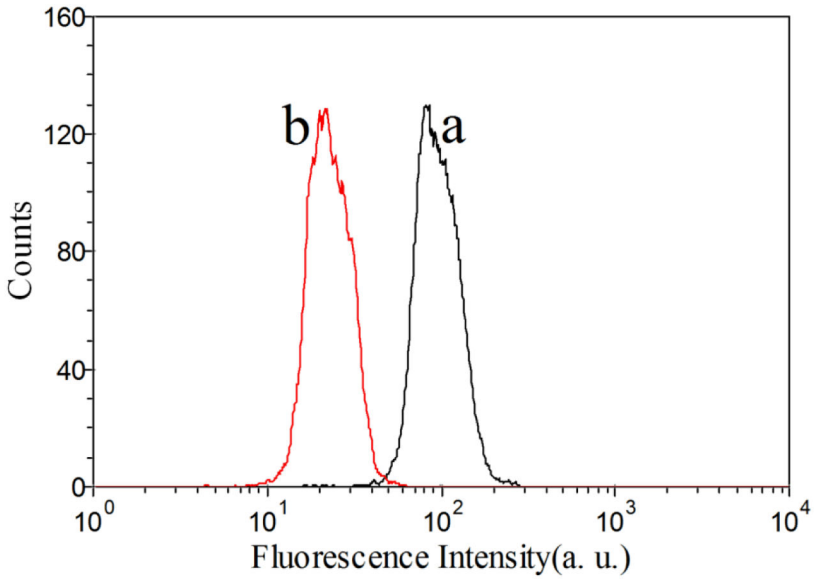

Fig. 7.

Flow cytometry histograms of doxorubicin under 37°C (a) and 4°C (b). A decreased DOX fluorescence intensity for cells incubated with S1-Dox at 4°C compared to that at 37°C indicated the lower cellular uptake of S1-Dox nanoparticles at 4°C